THE EVOLUTION OF THE MASS FUNCTION SPLIT BY MORPHOLOGY UP TO REDSHIFT 1 IN THE FORS DEEP AND THE GOODS-S FIELDS[1]

M. PANNELLA,[2] U. HOPP,[2,3] R. P. SAGLIA,[2] R. BENDER,[2,3] N. DRORY,[4] M. SALVATO,[2] A. GABASCH,[2,3] AND G. FEULNER[2,3]

ABSTRACT

We study the evolution of the stellar mass density for the separate families of bulge-dominated and disk-dominated galaxies over the redshift range $0.25 \leq z \leq 1.15$. We derive quantitative morphology for a statistically significant galaxy sample of 1645 objects selected from the FORS Deep Field and the GOODS-S field. We find that the morphological mix evolves monotonically with time: the higher the redshift, the more disk systems dominate the total mass content. At $z \sim 1$, massive objects ($M_* \geq 7 \times 10^{10}\ M_\odot$) host about half of the mass contained in objects of similar mass in the local universe. The contribution from early- and late-type galaxies to the mass budget at $z \sim 1$ is nearly equal. We show that in situ star formation is not sufficient to explain the changing mass budget. Moreover, we find that the star formation rate per unit stellar mass of massive galaxies increases with redshift only for the intermediate and early morphological types while it stays nearly constant for late-type objects. This suggests that merging and/or frequent accretion of small-mass objects has a key role in the shaping of the Hubble sequence as we observe it now and also in decreasing the star formation activity of the bulge-dominated descendants of massive disk galaxies.

Subject headings: cosmology: observations — galaxies: evolution — galaxies: formation — galaxies: fundamental parameters — galaxies: luminosity function, mass function — surveys

1. INTRODUCTION

Lilly et al. (1996) and Madau et al. (1996) produced the first estimates of the cosmic star formation history. Since then, the growing number of deep extragalactic surveys has allowed galaxy evolution to be tackled in greater detail, to higher and higher redshifts (e.g., Giavalisco et al. 2004; Gabasch et al. 2004b; Bouwens et al. 2004; Juneau et al. 2005). All these studies point toward a substantial amount of star formation at early cosmic epochs. Other works, mainly based on near-IR selected surveys like the Two Micron All Sky Survey (Cole et al. 2001), the Munich Near-IR Cluster Survey (Drory et al. 2004a), K20 (Fontana et al. 2004), the Faint Infrared Extragalactic Survey (Rudnick et al. 2003), the Hubble Deep Field (Dickinson et al. 2003), and the Great Observatories Origins Deep Survey (GOODS)+FORS Deep Field (FDF) (Drory et al. 2005), have been able to measure directly the stellar mass density up to high redshifts. The two independent approaches are in remarkably good agreement and suggest that about half of the present-day stars were already in place at $z \approx 1$, when the universe was half of its present age.

The assembly of the stellar mass through cosmic time is a crucial test for models of galaxy formation and evolution (Kauffmann & Charlot 1998). Such models aim at linking the hierarchical growth of dark matter structures to the observed galaxy properties, by means of simplified prescriptions for the formation of baryonic systems in dark matter halos (e.g., Cole et al. 2000; De Lucia et al. 2004). An effective way to constrain models is to understand where the stars were located, i.e., what was the morphology of their host galaxies, at different look-back times. This permits us to directly probe how galaxies assembled their stars and how their morphology (i.e., at least with some approximation, their dynamical status) evolves. Since merging is driving both mass assembly and dynamical evolution in a hierarchical scenario, these studies offer a direct probe of the role of this process in galaxy evolution.

Lacking sufficient angular resolution, galaxies have been classified, both at low and high redshift, as early or late types based on their broadband colors (Baldry et al. 2004; Fontana et al. 2004). This approach suffers, especially at high redshift, from the obvious drawback that a disk galaxy populated by an old stellar population would be classified as an early-type object (and vice versa). Bell et al. (2003) used the concentration parameter to discriminate between early- and late-type objects in a complete sample extracted from local surveys. They found that in the local universe the *transition mass*, i.e., the mass at which disks become dominant in the relative contribution to the total stellar mass function, is $\approx 5 \times 10^{10}\ M_\odot$.

In this work, we rely on a deep, complete, and automatically morphologically classified sample to study the contribution of galaxies of different morphologies to the redshift evolution of the stellar mass density. Bundy et al. (2005), and also Brinchmann & Ellis (2000), have carried out a work qualitatively similar to the one we present here but based on shallower samples and visual morphological classification.

This Letter is organized as follows: In § 2, we present the data set on which this work is based and the morphological analysis. In § 3, we discuss our results on the evolution of mass functions, mass densities, and specific star formation rates (SSFRs; i.e., star formation rate per unit stellar mass) split by morphological type. Finally, § 4 contains our conclusions. We use AB magnitudes and adopt a cosmology with $\Omega_M = 0.3$, $\Omega_\Lambda = 0.7$, and $H_0 = 70$ km s^{-1} Mpc^{-1}.

2. SAMPLE AND ANALYSIS

This study is based on photometric catalogs derived for the FDF (Heidt et al. 2003; Gabasch et al. 2004a) and part of the GOODS-

South (GOODS-S) field (M. Salvato et al. 2006, in preparation). The two fields cover approximately the same area (39.8 arcmin^2 for FDF and 50.6 arcmin^2 for GOODS-S). The FDF photometric catalog covers the *UBgRIzJKs* broad bands plus an intermediate band centered at 834 nm. The *I*-selected catalog used here lists 5557 galaxies down to $I_{lim} = 26.8$. For the GOODS-S field, our *K*-band–selected catalog contains 3240 galaxies, and it consists of *UBVRIJHK* broadband photometry (Arnouts et al. 2001; Schirmer et al. 2003; B. Vandame et al. 2006, in preparation). Number counts match the literature values down to $K_{lim} \approx 25$. Photometric redshifts are derived using the method described in Bender et al. (2001). Their accuracy is 3% and 5% for FDF and GOODS-S, respectively, with $\approx$1% outliers for both fields (for more details, see Gabasch et al. 2004a). For all galaxies in both catalogs, the *M/L* ratios were estimated with a log-likelihood–based spectral energy distribution (SED) fitting technique, using a library of SEDs built with the Bruzual & Charlot (2003) code, assuming a Salpeter (1955) initial mass function (IMF). The procedure used is described in detail in Drory et al. (2004b). We use here the same mass catalog as in Drory et al. (2005), so we refer the reader to this paper for more details.

Both the FDF and GOODS-S fields were imaged with the Advanced Camera for Surveys (ACS) on board the *Hubble Space Telescope* (*HST*). The FDF was imaged in the broadband F814W filter, with four Wide Field Channel pointings of 40 minutes exposure each, reaching a 10 σ limit of 26 mag. The data reduction was performed with the standard CALACS[5] pipeline, and the combined final mosaic was produced with the multi-drizzle package (Mutchler et al. 2002). The GOODS-S field was imaged in four different filters (*BVIz*) as part of the ACS GOODS legacy (Giavalisco et al. 2004); the 10 σ limit in the F775W band is 26.5 mag.

We use the publicly available packages GIM2D (Simard et al. 1999) and GALFIT (Peng et al. 2002) to fit point-spread function (PSF) convolved Sérsic (1968) profiles to the two-dimensional surface brightness of each object, down to a limit of F814W = 24 (FDF) and F775W = 24.5 (GOODS-S). The PSFs were obtained for each individual tile by stacking about 10 high signal-to-noise ratio isolated stars. The results from the two different codes are in excellent agreement, thus confirming the robustness both of our modeling and of the choice of flux limits. More details on the reduction and the data quality assessment, as well as on the whole fitting procedure and relative validation, will be described in M. Pannella et al. (2006, in preparation). In order to further check our morphological classification, visual morphology was performed by U. Hopp according to the de Vaucouleurs et al. (1991) classification scheme. A tight correlation is obtained between the average visual and automated classifications, parameterized by the morphological type T and the Sérsic index n_{Ser}, respectively (see Fig. 1). Using the visual or automated classification does not significantly affect the results presented in this study. We split our sample, according to the Sérsic index, into early-type ($n \geq 3.5$, $\approx T \leq -3$), intermediate ($2 \leq n < 3.5$, $\approx -3 < T \leq 2$) and late-type ($n < 2$, $\approx T > 2$). We evaluated the effect of morphological *k*-correction on this coarse classification scheme by also performing the surface brightness modeling on *B*- and *z*-band images for a subsample of the GOODS-S galaxies. We found that our broad classification is robust for objects at $z \leq 1.15$. Thus, we restrict our analysis to $z \leq 1.15$. Finally, we estimate the mass completeness of the two (FDF and GOODS-S) catalogs as the mass of a maximally old stellar population[6] having,
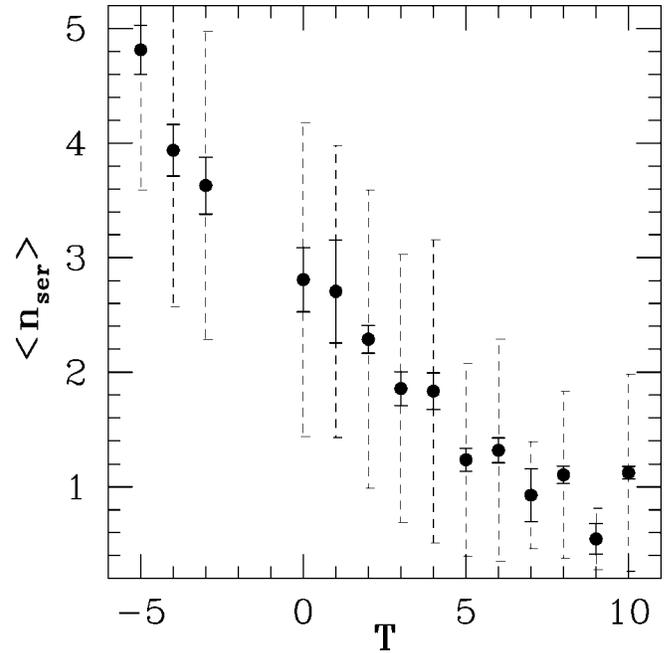
Fig. 1.—Correlation between the Sérsic index and the visual classification *T*-value for the GOODS-S subsample. Points are mean values. Solid error bars are the errors on the means, and dashed error bars show the rms values.

at every redshift, an observed magnitude equal to the catalog completeness magnitude (e.g., Dickinson et al. 2003). The final catalog contains 1645 galaxies.

3. THE SHAPING OF THE HUBBLE FORK UP TO REDSHIFT 1

We performed extensive Monte Carlo simulations to take into account the effect of mass uncertainties ($\approx$0.2 dex) on our results. Ten thousand simulations of the mass catalog were generated, perturbing each mass within a Gaussian of sigma equal to its error. Unless stated differently in the relevant figure captions, we use the median values of the Monte Carlo simulations in all figures. Error bars take into account both Poissonian errors on the median counts (Gehrels 1986), and 16th–84th percentile values of each distribution.

In Figure 2, we show the V/V_{max} corrected stellar mass functions, split by morphological type, in three redshift bins. The redshift intervals were chosen to have comparable numbers of objects in each bin. A dotted vertical line shows the mass completeness for each redshift bin. We find that, at all redshifts, the late-type objects dominate the low-mass end of the mass function, while the early- and intermediate-type objects dominate the high-mass end. In addition, Figure 2 shows that the relative contribution of disks to the high-mass end of the mass function increases with redshift. This suggests that (1) the morphological mix at the high-mass end evolves with redshift, and (2) the transition mass increases with redshift. The latter finding was already suggested in Bundy et al. (2005), but its significance was hampered by their mass completeness limit. In our case, the transition seems to happen well above the estimated mass completeness. As Figure 2 shows, at $z \sim 1$ the disks' and bulges' contributions become comparable at $\approx 1 \times 10^{11}$ $M_\odot$.

In order to better explore the evolution of the morphological mix at the high-mass end, we cut the three subsamples at the same common mass completeness ($M_* \geq 7 \times 10^{10}$ $M_\odot$) hereafter. This guarantees a fair comparison between the three redshift bins. The top panel of Figure 3 shows the behavior of the ratio of the number densities of bulges and disks. At increasing red-
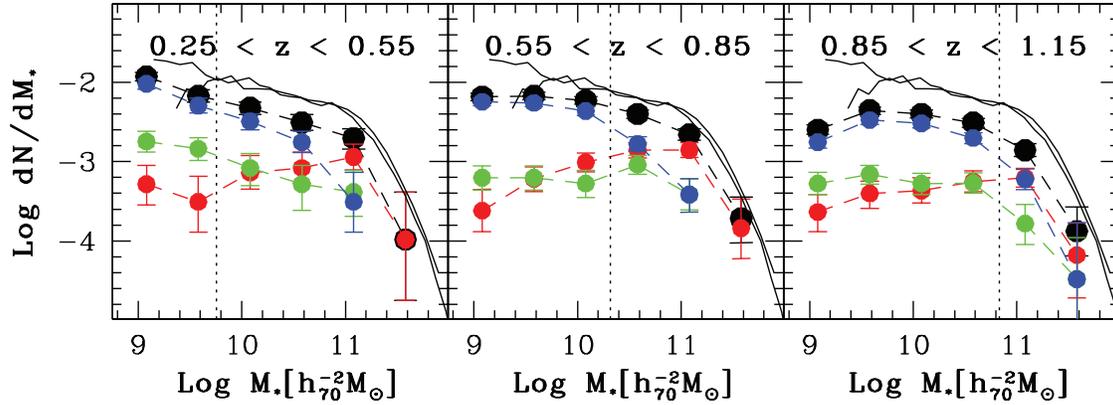
Fig. 2.—Mass function split by morphological types (early in red, intermediate in green, and late in blue) in three redshift bins. Black symbols refer to total values. The vertical axis is in units of h_{70}^3 Mpc^{-3} dex^{-1}. The vertical dotted line indicates the mass completeness limit in each redshift bin. Dashed colored lines are intended to guide the eye. Solid black lines show the local mass function determinations from Cole et al. (2001) and Bell et al. (2003).

shift, this ratio is found to systematically decrease with respect to the no-evolution hypothesis at more than $3\,\sigma$ significance. In the bottom panel of Figure 3, we show the stellar mass density split by morphological type at different redshifts. The error estimates of the total values include the cosmic variance contribution, estimated as in Somerville et al. (2004). In agreement with previous studies (see § 1), we find that at $z \sim 1$ massive objects host almost half of the stellar mass contained in similarly massive objects at $z = 0$. In addition, we find that the contribution to the total mass budget from early- and late-type galaxies is almost equal at $z \sim 1$ but strongly evolves with redshift: there is a *mass pouring* from disk systems to bulge-dominated objects.

Our findings require a scenario in which massive objects al-

most double their mass from redshift 1 to 0 and become more and more bulge-dominated systems as time goes by. A possibility is that in situ star formation increases the mass and secular evolution modifies the morphology (Kormendy & Kennicutt 2004). Under simplified assumptions, we can estimate whether the star formation rates (SFRs) of the galaxies in our three redshift subsamples can account for a doubling of the stellar mass by $z = 0$. Following Madau et al. (1998), the SFR of individual objects can be estimated from the rest-frame UV luminosity as SFR$_{2800} = 1.27 \times 10^{-28} \times L_{2800}$ in units of $M_\odot$ yr^{-1}, where the constant factor is computed for a Salpeter IMF. We apply a dust attenuation correction of $A_{2800} = 1$ mag to the whole sample. This median value, assumed not to depend on redshift, is derived as in Gabasch (2004) by comparing the total stellar mass density and the integral of the SFR density at different lookback times. Figure 4 shows the median SSFR values for the three redshift bins and for the different morphological types, cut at the same mass completeness as described above. Since it is not possible to know the individual star formation histories, we derive the median SFR decline with cosmic time from the massive galaxies subsample, and we assume that all the objects in our
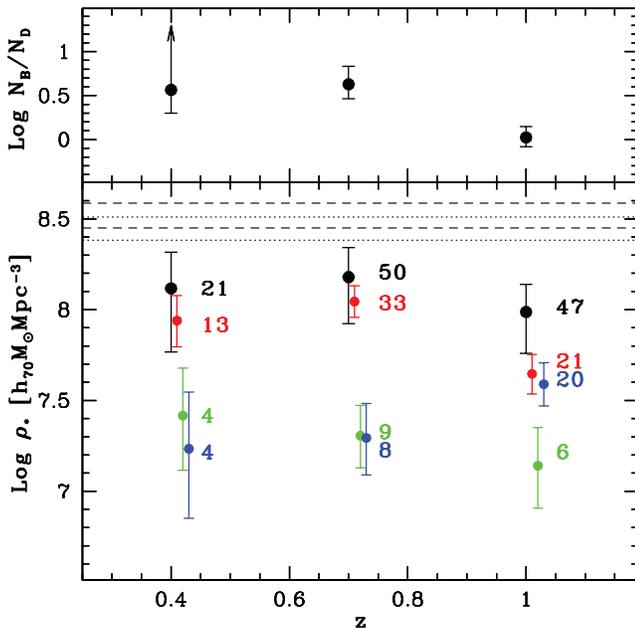

Fig. 3.—*Top panel*: Redshift evolution of the ratio of bulge and disk number densities. Error bars show the 5th and 95th percentiles of the ratio distributions. *Bottom panel*: Stellar mass densities for objects with $M_* \geq 7 \times 10^{10}\ M_\odot$ (color coding according to galaxy morphology, as in Fig. 2). Points are slightly shifted in redshift for clarity. The median numbers of objects in each class are also labeled. Error bars account for Poissonian errors, mass uncertainties, and cosmic variance (for the total values only) as described in the text. Dotted and dashed lines indicate the $3\,\sigma$ range estimate obtained at redshift 0, with the same mass cut and IMF, from Cole et al. (2001) and Bell et al. (2003), respectively.
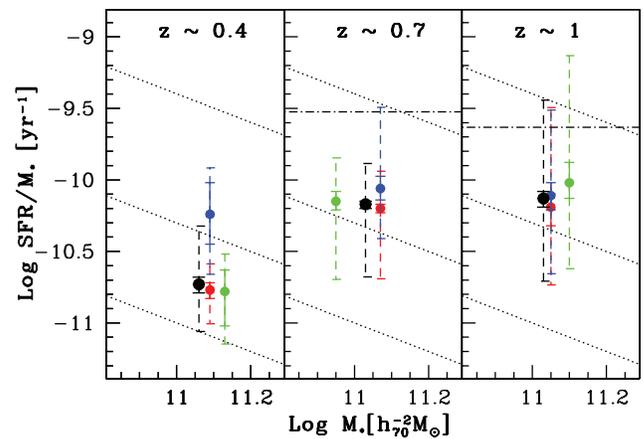

Fig. 4.—Median SSFR for different morphological types. The colored symbols (same color coding as in previous figures) show the median values in both stellar mass and SSFR. Dashed error bars represent the median 10th and 90th percentiles of the Monte Carlo realizations, while the solid error bars show $1\,\sigma$ uncertainties on the median values. Tilted lines are constant SFR values (*from the bottom*: 1, 5, 40 $M_\odot$ yr^{-1}), while the horizontal lines mark the doubling mass lines (only for the last two redshift bins; see text for details).

sample follow this median star formation history. In this way, we can estimate, at every redshift, the minimum SSFR that enables an object to double its mass by $z = 0$. These minimum SSFRs are shown in the plot as horizontal lines at the last two redshift bins considered. It appears that only a small fraction of the $z \sim 1$ sample would be able to double its mass. An alternative and more likely solution (see also Brinchmann & Ellis 2000) is a continuous accretion of smaller mass galaxies, and possibly the merging of massive disks, which can account for both the changing total mass budget and the morphological mix evolution.

In the past, a number of works (e.g., Brinchmann & Ellis 2000; Feulner et al. 2005a, 2005b; Bauer et al. 2005) have focused on the SSFR redshift evolution and consistently found an increase of the SSFRs with redshift. Hence, the bulk of star formation in massive galaxies was pushed to $z \geq 2$, in agreement with the downsizing scenario (Cowie et al. 1996). Here for the first time we explore the SSFR evolution split by different morphological types. We find, for objects with $M_* \geq 7 \times 10^{10}\, M_\odot$, a different behavior in the SSFR redshift evolution for the different morphological types. The median SSFR of late-type objects shows only a mild, if any, evolution up to $z \sim 1$, while the median values of early and intermediate types are clearly increasing with redshift. Since these latter populations are dominating in numbers, they drive the redshift evolution of the whole massive galaxy distribution. This finding, together with the previous arguments, suggests that the morphological evolution of massive disk galaxies toward more and more bulge-dominated systems is accompanied by a decrease in the SSFR of their end products. Bell et al. (2005) show that a large part of the star formation in massive galaxies at $z \sim 0.7$ is due to normal spiral galaxies. Moreover, they conclude that turning off star formation in these objects is responsible for the observed decline of cosmic star formation thereafter. We find a good agreement at $z \sim 0.7$ with their result but also a hint that the decline of star formation in massive galaxies is linked more to the evolution of bulge-dominated galaxies.

4. CONCLUSIONS

In this Letter, we have studied the contribution of disks and bulges to the evolution of the stellar mass function up to $z \sim 1$.

We agree with Bundy et al. (2005) that the transition mass, i.e., the mass at which disks become dominant in the relative contribution to the total mass function, increases with redshift. We estimate that at $z \sim 1$ the transition mass is up to a factor of 2 larger than its measured local value.

We show that the morphological mix evolves with redshift. At $z \sim 1$, early- and late-type galaxies contribute nearly equally to the total mass budget in massive objects (i.e., with $M_* \geq 7 \times 10^{10}\, M_\odot$). We suggest that merging events must play a key role in the *mass pouring* from disks to bulges.

We find a different behavior of the SSFR, i.e., the star formation rate per unit stellar mass, as a function of redshift for the different morphological types. The median SSFR of late-type objects shows almost no evolution up to $z \sim 1$. Conversely, median SSFRs for early and intermediate types increase systematically. Since these latter morphological types are dominating in numbers, they drive the total SFR evolution of massive galaxies. This suggests a scenario where the morphological evolution of massive disk galaxies through merging is followed by the decrease of the star formation in their bulge-dominated descendants, maybe after a burst of star formation that exhausts the available gas.

REFERENCES

Arnouts, S., et al. 2001, A&A, 379, 740
Baldry, I. K., Glazebrook, K., Brinkmann, J., Ivezić, Ž., Lupton, R. H., Nichol, R. C., & Szalay, A. S. 2004, ApJ, 600, 681
Bauer, A. E., Drory, N., Hill, G. J., & Feulner, G. 2005, ApJ, 621, L89
Bell, E. F., McIntosh, D. H., Katz, N., & Weinberg, M. D. 2003, ApJS, 149, 289
Bell, E. F., et al. 2005, ApJ, 625, 23
Bender, R., et al. 2001, in Deep Fields, ed. S. Cristiani, A. Renzini, & R. E. Williams (Berlin: Springer), 96
Bouwens, R. J., et al. 2004, ApJ, 606, L25
Brinchmann, J., & Ellis, R. S. 2000, ApJ, 536, L77
Bruzual, G., & Charlot, S. 2003, MNRAS, 344, 1000
Bundy, K., Ellis, R. S., & Conselice, C. J. 2005, ApJ, 625, 621
Cole, S., Lacey, C. G., Baugh, C. M., & Frenk, C. S. 2000, MNRAS, 319, 168
Cole, S., et al. 2001, MNRAS, 326, 255
Cowie, L. L., Songaila, A., Hu, E. M., & Cohen, J. G. 1996, AJ, 112, 839
De Lucia, G., Kauffmann, G., & White, S. D. M. 2004, MNRAS, 349, 1101
de Vaucouleurs, G., de Vaucouleurs, A., Corwin, H. G., Jr., Buta, R. J., Paturel, G., & Fouqué, P. 1991, Third Reference Catalogue of Bright Galaxies (Berlin: Springer)
Dickinson, M., Papovich, C., Ferguson, H. C., & Budavári, T. 2003, ApJ, 587, 25
Drory, N., Bender, R., Feulner, G., Hopp, U., Maraston, C., Snigula, J., & Hill, G. J. 2004a, ApJ, 608, 742
Drory, N., Bender, R., & Hopp, U. 2004b, ApJ, 616, L103
Drory, N., Salvato, M., Gabasch, A., Bender, R., Hopp, U., Feulner, G., & Pannella, M. 2005, ApJ, 619, L131
Feulner, G., Gabasch, A., Salvato, M., Drory, N., Hopp, U., & Bender, R. 2005a, ApJ, 633, L9

Feulner, G., Goranova, Y., Drory, N., Hopp, U., & Bender, R. 2005b, MNRAS, 358, L1
Fontana, A., et al. 2004, A&A, 424, 23
Gabasch, A. 2004, Ph.D. thesis, Ludwig-Maximilians-Universität, München
Gabasch, A., et al. 2004a, A&A, 421, 41
———. 2004b, ApJ, 616, L83
Gehrels, N. 1986, ApJ, 303, 336
Giavalisco, M., et al. 2004, ApJ, 600, L93
Heidt, J., et al. 2003, A&A, 398, 49
Juneau, S., et al. 2005, ApJ, 619, L135
Kauffmann, G., & Charlot, S. 1998, MNRAS, 297, L23
Kormendy, J., & Kennicutt, R. C., Jr. 2004, ARA&A, 42, 603
Lilly, S. J., Le Fèvre, O., Hammer, F., & Crampton, D. 1996, ApJ, 460, L1
Madau, P., Pozzetti, L., & Dickinson, M. 1998, ApJ, 498, 106
Madau, P., Ferguson, H. C., Dickinson, M. E., Giavalisco, M., Steidel, C. C., & Fruchter, A. 1996, MNRAS, 283, 1388
Mutchler, M., Koekemoer, A. M., & Hack, W. 2002, in The 2002 *HST* Calibration Workshop, ed. S. Arribas, A. Koekemoer, & B. Whitmore (Baltimore: STSI), 70
Peng, C. Y., Ho, L. C., Impey, C. D., & Rix, H.-W. 2002, AJ, 124, 266
Rudnick, G., et al. 2003, ApJ, 599, 847
Salpeter, E. E. 1955, ApJ, 121, 161
Schirmer, M., et al. 2003, A&A, 407, 869
Sérsic, J. L. 1968, Atlas de Galaxias Australes (Cordoba: Obs. Astron.)
Simard, L., et al. 1999, ApJ, 519, 563
Somerville, R. S., Lee, K., Ferguson, H. C., Gardner, J. P., Moustakas, L. A., & Giavalisco, M. 2004, ApJ, 600, L171